Accepted Manuscript

Thermo-oxidative stabilization of poly(lactic acid) with antioxidant intercalated layered double hydroxides

Lucía Pérez Amaro, Francesca Cicogna, Elisa Passaglia, Elisabetta Morici, Werner Oberhauser, Sahar Al-Malaika, Nadka Tz Dintcheva, Serena Coiai

PII: S0141-3910(16)30243-9

DOI: 10.1016/j.polymdegradstab.2016.08.005

Reference: PDST 8031

To appear in: *Polymer Degradation and Stability*

Received Date: 26 July 2016

Accepted Date: 11 August 2016

Please cite this article as: Amaro LP, Cicogna F, Passaglia E, Morici E, Oberhauser W, Al-Malaika S, Dintcheva NT, Coiai S, Thermo-oxidative stabilization of poly(lactic acid) with antioxidant intercalated layered double hydroxides, *Polymer Degradation and Stability* (2016), doi: 10.1016/j.polymdegradstab.2016.08.005.

Thermo-oxidative stabilization of poly(lactic acid) with antioxidant intercalated layered double hydroxides

Lucía Pérez Amaro[1], Francesca Cicogna[1], Elisa Passaglia[1], Elisabetta Morici[3], Werner Oberhauser[2], Sahar Al-Malaika[4], Nadka Tz. Dintcheva[3], Serena Coiai[1*]

[1]Istituto di Chimica dei Composti Organo Metallici (ICCOM), Consiglio Nazionale delle Ricerche, UOS Pisa, Via G. Moruzzi 1, 56124 Pisa, Italy

[2]Istituto di Chimica dei Composti Organo Metallici (ICCOM), Consiglio Nazionale delle Ricerche, Via Madonna del Piano 10, 50019 Sesto Fiorentino (FI), Italy

[3]Dipartimento di Ingegneria Civile, Ambientale, Aerospaziale, dei Materiali, Università di Palermo, Viale delle Scienze, Ed. 6, 90128 Palermo, Italy

[4]Aston University, Aston Triangle, Polymer Processing & Performance Research Unit, Birmingham B4 7ET, United Kingdom

*Corresponding author e-mail: serena.coiai@pi.iccom.cnr.it

Abstract

Two antioxidant modified layered double hydroxides (AO-LDHs) were successfully prepared by the intercalation of 3-(3,5-di-tert-butyl-4-hydroxyphenyl)propionic acid (IrganoxCOOH) and 6-hydroxy-2,5,7,8-tetramethylchroman-2-carboxylic acid (Trolox) in the layered structure of LDH. It was found that by anchoring the phenolic moieties to the LDH layers the antioxidant power is retained in the case of Trolox, and even amplified in the case of IrganoxCOOH. A small amount of the two AO-LDHs was incorporated into poly(lactic acid), PLA, by solution mixing and melt extrusion. The thermo-oxidative stability of the composites was compared with that of the neat PLA and PLA containing free AOs. SEC analysis indicates that, after a controlled period of ageing, both the AO-LDHs protect the PLA from chain scission. The oxidation induction time (OIT, DSC) at 230 °C shows also the beneficial effects of the presence of the functional filler in the polymer matrix. Further, results from a preliminary migration test suggest that the AO species have a low tendency to migrate away from the AO-LDHs embedded in the polymer matrix thus keeping the AO protected inside the nanofiller layers thereby remaining active for a longer time.

Keywords: antioxidants, layered double hydroxides (LDHs), poly(lactic acid), thermo-oxidative degradation

1. Introduction

Polymers are normally exposed to thermo- and photo-oxidative degradation during both processing and service life, affecting their performance, especially for long-term applications [1, 2]. To avoid or retard the oxidative degradation process, low concentration (0.05-0.5 wt.%) of antioxidants (AOs), such as hindered phenols or amines and organophosphorus compounds, are typically added to polymers [3].

Even though the chemistry of AOs is now well known, there remain a number of issues including problems related to poor thermal stability of AOs, their migration from the bulk to the surface, their deactivation by reactions with other chemicals, and eventual toxicity particularly for food contact packaging applications. In particular, physical loss of AOs is promoted by their volatilization, poor solubility and migration. To overcome this problem, high molecular weight AOs have been used; however, the poor solubility of such AOs and their physical loss by leaching due to aggressive service conditions are open challenges [4-6]. The covalent attachment of AO moieties onto a polymer backbone as well as their immobilization into a host solid support are considered as alternative approaches to reduce their physical loss. The polymerization of hindered phenol bearing monomers [7], the copolymerization of ethylene with AO functionalized norbornene [8], and the free radical grafting of mono and bis-acrylate/methacrylate and maleimide substituted with hindered phenols or sterically hindered amines onto polyolefins are successful examples of macromolecular AOs preparation and grafting of AOs [9-13]. The extraction resistance of such AOs by solvent media is dramatically improved even if the antioxidant efficiency decreases, presumably due to the low mobility of these AOs.

Among the host-guest methods, AOs have been successfully grafted on nanosilica particles and then dispersed in polyolefins to demonstrate their antioxidant ability [4, 14, 15]. It was shown that the antioxidant efficiency of the nanosilica-immobilized AO particles is improved with respect to the corresponding low molecular AOs and high stability is retained against migration. Similarly, AO-containing organo-modified montmorillonite [16] and AO modified carbon nanotubes [17, 18] have been prepared and compounded with polymers. Layered double hydroxides (LDHs) have been also proposed as host matrix. LDHs are inorganic solids made of positively charged and pillared hydroxide lamellae balanced by interlayer anions, which can be easily exchanged with organic anions thus

increasing the basal spacing and improving compatibility with polymer matrices [19-21]. LDHs are excellent host matrices for storage and delivery of bioactive molecules and drugs, which are in this way protected against degradation by light, temperature, oxygen, alkali metals, etc. [22-24, 25]. LDHs have been specifically used as nanocarriers of AOs, such as carnosine, gallic acid, vanillic acid, and ferulic acid [26, 27]. The intercalation between the layers protects the AO from oxidation during storage [22, 24], reduces the effects of migration, and shows release behaviour suitable for their use in controlled delivery systems [22]. Similarly, trans-cinnamic derivatives (ferulic acid, cafeic acid, hydroxycinnamic acid), known as AOs and UV blockers, have been successfully entrapped between LDH layers for cosmetic use as UV sunscreens and UV stabilizers [28]. Recently, 3-(3,5-di-tert-butyl-4-hydroxyphenyl)propionic acid, containing the 2,6-di-tert-butylphenol functional group that is one of the most used AO in industry, has been intercalated within LDH galleries through co-precipitation [29] and regeneration method [30, 31]. The modified LDH has been dispersed in polypropylene (PP) [29, 30]. Thermo-mechanical properties as well as thermo- and photo-oxidative resistance of composites were evaluated demonstrating that the AO-intercalated LDH enhances the long-term performance of PP composites.

Poly(lactic acid) (PLA) is an emerging polymer from renewable sources, having good thermoplastic behaviour, good processability and fulfilling biodegradable requirements and, for these reasons, is considered an interesting candidate to replace more traditional materials like polyolefins in different industrial applications (packaging, films for agro-industry, fibers etc.). However, PLA performance in terms of durability are limited by multiple chemical ageing mechanisms, such as hydrolysis, thermal decomposition, photo-oxidation under natural weathering conditions and thermo-oxidation at high temperature which is an important issue considering the processing methodologies [32]. In particular, PLA degradation at the normal processing temperature (around 200 °C) follows a random chain scission mechanism determining a significant level of molecular degradation and polymer embrittlement. It is reported that under these conditions, acyl-O and alkyl-O β-C initiated homolytic chain-scission can occur as well as radical reactions induced by oxygen, thus determining random chain cleavage and leading to formation of linear hydroxyl and carboxyl terminated species [33]. In a recent study, it has been also demonstrated that the oxidative degradation of PLA at moderate temperatures (below PLA melting temperature) follows a radical pathway [32] with a significant reduction of the polymer molar mass.

The aim of the present study is to determine the influence of stabilised-LDHs, that have been intercalated with two different hindered phenolic antioxidant functions (AO-LDH), on the

thermoxidative stability of PLA-LDH nanocomposites prepared by both solution mixing and melt extrusion. The intercalation of the AO-molecules and their amount in the hybrid system, as well as, the free radical antioxidant activity of the resulting AO-LDH are discussed (the latter examined using DPPH, 2,2-diphenyl-1-picrylhydrazyl, assay [34]) and the migration of the intercalated-AO moieties from PLA composites is also addressed.

The antioxidant-modified LDHs (AO-LDHs) were prepared by intercalation between the inorganic layers via anion exchange of 3-(3,5-di-tert-butyl-4-hydroxyphenyl)propionic acid (IrganoxCOOH) and 6-hydroxy-2,5,7,8-tetramethylchroman-2-carboxylic acid (Trolox), a water-soluble analogue of vitamin E (Scheme 1), respectively. The oxidation induction time (OIT) was determined by differential scanning calorimetry (DSC).

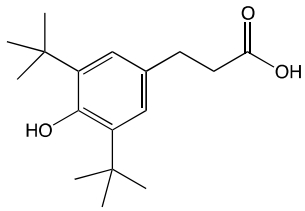

IrganoxCOOH

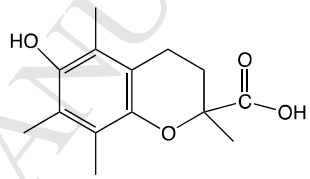

Trolox

Scheme 1. Chemical structure of 3-(3,5-di-tert-butyl-4-hydroxyphenyl)propionic acid (IrganoxCOOH) and 6-hydroxy-2,5,7,8-tetramethylchroman-2-carboxylic acid (Trolox)

2. Experimental

2.1 Materials

Poly(lactic acid) (PLA) Ingeo^{TM} Biopolymer 2003D 96% L-lactide produced by NatureWorks®, USA, MFI (2.16 kg/190 °C) 4 - 8 g/10 min was used as polymer matrix. PLA was dried in a vacuum oven for 18 h at 110 °C before use. Pural MG63HT, a magnesium aluminum hydroxy carbonate (LDH-CO_3), with the molecular formula $Mg_{0.66}Al_{0.34}(OH)_2(CO_3)_{0.17}\cdot 0.62H_2O$ as previously determined [35] and Perkalite F100S [36], a magnesium aluminum LDH modified with hydrogenated fatty acids (organo-LDH, containing 55 wt.% of stearate and palmitate), were kindly supplied by Sasol Germany GmbH and Akzo Nobel, respectively. The octadecyl-3-(3,5-di-*tert*-butyl-4-hydroxyphenyl)propionate (Irganox 1076, ex. Ciba Specialty Chemicals, BASF) was hydrolyzed to obtain the 3-(3,5-di-tert-butyl-4-

hydroxyphenyl)propionic acid (IrganoxCOOH) [37]. 6-Hydroxy-2,5,7,8-tetramethylchroman-2-carboxylic acid (Trolox, Sigma-Aldrich), 3,5-di-*tert*-4-butylhydroxytoluene (BHT, Sigma-Aldrich), free radical 2,2-diphenyl-1-picrylhydrazyl hydrate (DPPH, Sigma-Aldrich), methanol (Sigma-Aldrich), chloroform (Carlo Erba, RPE grade), and chloroform (Sigma-Aldrich, HPLC grade, ≥99.8%, ethanol stabilized) were used without further purification.

2.2 Preparation of the antioxidant intercalated LDHs (AO-LDHs)

LDH-CO_3 was first converted into the nitrate form (LDH-NO_3) according to the titration procedure reported by Muksing *et al.* [21]. LDH-CO_3 was dispersed in a 1 M $NaNO_3$ aqueous solution (mass/volume = 2 g/100 ml) and the suspension was titrated with a 1 M HNO_3 solution. After titration, the white solid was washed several times with CO_2-free deionized water and dried overnight at 60 °C in a vacuum oven. The calculated anion-exchange capacity (AEC) of LDH-NO_3 having the formula $Mg_{0.66}Al_{0.34}(OH)_2(NO_3)_{0.34}\cdot 0.44H_2O$ (determined according to the analytic procedure described in Ref. [21]) is 3.85 mmol of NO_3^-/g, calculated as follows: $AEC = x/Mw\cdot 10^3$ (mequiv/g), where Mw and x are the molecular weight and the layer charge per octahedral unit, respectively. The AO-LDHs were then obtained by anion exchange. An amount of AO corresponding to 1.5 times the AEC of the LDH-NO_3 was dissolved in 300 ml of CO_2-free deionized water and heated at 70 °C. A NaOH 1M solution was added drop wise until pH= 9 (for IrganoxCOOH) and pH= 6 (for Trolox) were reached. Once the antioxidant was completely solubilized at the target pH values, 1 g of LDH-NO_3 was added to the solution under nitrogen atmosphere, and then kept under stirring for three days in dark conditions at 70 °C. Both AO-LDHs, labelled as IrganoxCOOH-LDH and Trolox-LDH, were recovered by filtration, washed several times with deionized CO_2-free water until pH=7, and finally dried under vacuum at 60 °C to constant weight.

2.3 Preparation of the PLA/AO-LDH composites

PLA/IrganoxCOOH-LDH and PLA/Trolox-LDH composites, containing 0.50 wt.% of AO-LDH with respect to the polymer matrix, were first prepared by solution mixing (labelled as S) followed by film casting. In a typical experiment, the AO-LDH was first suspended in a chloroform/methanol 70/30 (v/v) solution, stirred and sonicated for 20 min. The AO-LDH dispersion was observed by exposing the suspension to a red beam and, in accordance with the Tyndall effect, a continuous red laser line across the suspension was observed for both the samples which was taken to indicate the occurrence of a delaminated morphology [38, 39]. Subsequently, the suspension containing the hybrid filler was added

to a PLA chloroform solution (1.5 g of PLA per 60 ml of $CHCl_3$) and kept under stirring for 1 h at room temperature. A film of the composite was then obtained by solution casting and dried under vacuum at 60 °C for 24 h until constant weight. For comparison, films were also prepared for the neat PLA and PLA-containing the free AO species (IrganoxCOOH and Trolox) as well as films of PLA with the organophilic LDH Perkalite F100S (Table 1).

PLA/AO-LDH composites containing 0.50 wt.% of AO-LDH were also prepared by melt extrusion (labelled as E). The two composites were processed in a Haake Minilab Micro Compounder model CTW5 fitted with a co-rotating twin-screw conical extruder. The extrusions were performed at 170°C, screw speed of 100 rpm, and the residence time was 5 min. Then the extrudates were pelletized, and thin nanocomposite films were prepared by compression moulding with a Carver 12 Ton Hydraulic Units, model 3912, working at 170°C.

Later films of all the samples obtained by solution mixing and melt extrusion were aged at 200°C in a ventilated air oven for different times (1, 3 and 6 hours). At the end of the ageing treatment, samples were analyzed by SEC.

Table 1. PLA/AO-LDH composites and reference samples prepared by solution mixing (S) and melt extrusion (E)

Sample	LDH[a] (wt %)	Free AO[b] (wt %)
PLA/IrganoxCOOH-LDH (S)	0.50	−
PLA/Trolox-LDH (S)	0.50	−
PLA/organo-LDH (S)	0.50	−
PLA/IrganoxCOOH-LDH (E)	0.50	−
PLA/Trolox-LDH (E)	0.50	−
PLA/IrganoxCOOH (S)	−	0.14
PLA/Trolox (S)	−	0.13

[a]The quantity of AO-LDH and organo-LDH was calculated as percentage of the hybrid system with respect to the polymer.
[b]The free AOs were added in equal amount with respect to the AO species contained in the PLA/AO-LDH samples.

2.4 Characterization

Wide-angle X-ray diffraction (WAXD) analysis was performed at room temperature with a X'Pert PRO (PANalytical) powder diffractometer in the 1.5 - 30° 2θ range at the scanning rate of 0.016°/min,

using a Cu Kα radiation (1.5406 Å). The interlayer spacing between the LDH layers, d_{003}, was computed by applying the Bragg's law.

Infrared spectra were recorded with a Fourier Transform Spectrometer PerkinElmer Spectrum 100 over the wavenumber range of 450 - 4000 cm^{-1}. The spectra of LDHs as well as those of the AOs were obtained by mixing the samples with potassium bromide (KBr 99.4% spectroscopic grade purchased from Sigma-Aldrich).

Thermogravimetric analysis (TGA) was performed using an Exstar TG/DTA Seiko 7200 instrument. Samples (5-10 mg) were placed in alumina sample pans and runs were carried out at the standard rate of 10 °C min^{-1} from 30 to 900 °C under air flow (200 mL min^{-1}).

Number average molecular weight (M_n) and weight average molecular weight (M_w) as well as dispersity (M_w/M_n) were determined using size exclusion chromatography (SEC). The system used is an Agilent Technologies 1200 Series comprising a degasser, an isocratic HPLC pump, a refractive index (RI) detector, and two PLgel 5 μm MiniMIX-D columns conditioned at 35 °C using chloroform ($CHCl_3$) as the mobile phase at a flow rate of 0.3 mL min^{-1}. The system was calibrated with polystyrene standards in a range from 500 to 3×10^5 g mol^{-1}. Samples were dissolved in $CHCl_3$ (2 mg mL^{-1}) and filtered through a 0.20 micron syringe filter before analysis. Number average molecular weight (M_n) and weight average molecular weight (M_w) were calculated using the Agilent ChemStation software. All SEC measurements were performed in triplicate. The values in Table 3 are approximate values of averaged values and the standard deviation is for all about 5% of the value.

UV-Vis absorption spectra were recorded at room temperature with a Perkin-Elmer Lambda 25 UV-Vis Spectrometer.

Oxidation induction time (OIT) measurements were performed using a differential scanning calorimeter DSC 4000 (Perkin-Elmer). Measurements were performed on disk-shaped specimens having a thickness ranging from 0.20 to 0.45 mm and weight around 5 – 10 mg. Samples were isothermally treated at 30 °C under nitrogen flow (50 mL min^{-1}) for 5 min, then they were heated from 30 °C to 230 °C at 20 °C/min under nitrogen flow (50 mL min^{-1}). After maintaining in nitrogen for 5 min to attain thermal equilibrium, the gas was switched to oxygen flow (50 mL min^{-1}). The OIT was determined from the onset of the exothermic oxidation reaction of PLA shown in the calorimetric curves. Five determinations were done for each sample and the OIT average number was reported.

Bright field transmission electron microscopy (TEM) experiments were performed on thin films using a FEI TECNAI G12 Spirit-Twin (120 kV, LaB6) microscope equipped with a FEI Eagle 4k CCD

camera (Eindhoven, The Netherlands). Thin sections of the samples (nominal thickness 100 nm) were cut using a Leica UC7 ultramicrotome (Wien, Austria) and placed on 400 mesh copper grids.

The rheological characterization was performed using a Rheometric Scientific (USA) RDA II plate-plate rotational rheometer, at T = 170°C and strain deformation at 5%; this latter was chosen after that amplitude sweeps were performed to ensure that the dynamic tests were in the linear viscoelasticity region. The complex viscosity (η*) and the storage (G') and loss (G'') moduli were recorded as a function of frequency in the range 0.1-100 rad/sec.

2.5 Assessment of the antioxidant activity of AO-LDHs

The radical scavenging activity of AO species and AO-LDHs was determined according to the DPPH method [34, 24, 29, 31]. A 25 mL methanol stock solution of DPPH (60 μM) was prepared and the related UV-Vis spectrum was recorded as reference. In the case of the pure antioxidants (BHT, IrganoxCOOH, and Trolox), their stock solutions were prepared by solubilizing an amount of the AO (about 5 mg) in 2 mL of MeOH and then solutions at different concentration (ranging between 6×10^{-5} M and 4×10^{-6} M) were prepared by diluting the appropriate aliquots of the stock. Later, for each AO diluted solution, 80 μL was added to 3 mL of the DPPH stock solution and the kinetic assay was followed immediately by UV-Vis spectroscopy by monitoring continuously the absorbance at 516 nm. For each sample the analysis was repeated three times, and average values of parameters as well as standard deviation were reported.

For comparison also a solution of DPPH in the absence of other additives was also analysed during time. In the case of organo-LDH and AO-LDHs (IrganoxCOOH-LDH and Trolox-LDH), the stable stock suspensions were prepared by ultrasound-assisted dispersion (5 - 10 min at medium frequency) of the hybrid filler in MeOH (about 5 mg in 2 mL of MeOH). Subsequently, aliquots of 80, 40, 20, and 10 μl, were added separately to 3 mL of the stock DPPH solution and the absorbance at 516 nm of the resulting suspension was recorded. In the case of the organo-LDH only the first dilution was followed during time. In all cases, the absorbance values were recorded as a function of time until a steady state was achieved, i.e. no further change in the absorbance. The percentage of DPPH remaining at the steady state was plotted against the AO/DPPH molar ratio, taking into account that, in the case of AO-LDH, the concentration of AO used in the DPPH solution corresponds to that of the organic amount present as determined from the TGA measurements. The effective concentration (EC_{50}) value, i.e. the concentration of the AO needed to decrease the initial concentration of DPPH radical by 50%, was determined from these plots.

The percentage of the remaining DPPH at the steady state was calculated as follows:

$$\%\ of\ remaining\ DPPH\ at\ the\ steady\ state = (Abs_{st}/Abs_0) \cdot 100\%$$

where Abs_0 and Abs_{st} are the absorbance of the solution at the time 0 and at the steady state, respectively. The antiradical power (ARP), taken as $1/EC_{50,}$ was also calculated as well as the stoichiometric value, which represents the number of moles of DPPH reduced by 1 mole of AO and calculated as $1/(2 \times EC_{50})$.

2.6 Migration test

The release of AO moieties from PLA/AO-LDH composites and PLA/AO physical blends obtained by solution mixing was investigated preliminarily by migration tests. The migration test was performed by immersing films of the samples (0.75 cm^2 of contact area per 1.5 mL of liquid) in ethanol (RPE grade 96%)/water 95/5 v/v solution at 40°C for 24 h [40]. Then, after the contact time elapsed, the films were recovered and dried. After migration, all the samples were analyzed by DSC for determining the OIT values following the same procedure previously described.

3. Results and discussion

3.1 Structural and chemical properties of the AO-LDHs

Two different AO-LDHs were prepared and compared: IrganoxCOOH-LDH and Trolox-LDH. The successful intercalation via anion exchange of the AO species between the LDH sheets was confirmed by WAXD and FT-IR. The mean interlayer spacing of IrganoxCOOH-LDH and Trolox-LDH determined from the WAXD patterns (Figure 1) is 2.60 nm ($2\theta = 3.4°$) and 1.73 nm ($2\theta = 5.1°$), respectively, whereas the precursor LDH-NO_3 has a basal spacing of 0.89 nm corresponding to a sharp (003) reflection at $2\theta = 9.9°$. Higher order reflection peaks (00l) evidencing the formation of well-ordered AO intercalated LDH layers were observed for both IrganoxCOOH-LDH and Trolox-LDH.

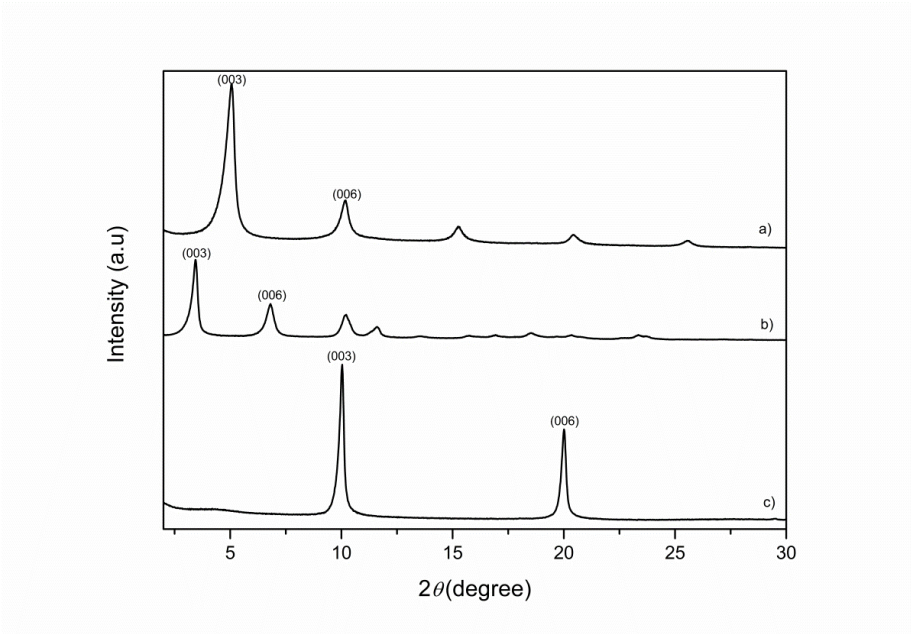

Figure 1. WAXD patterns of the Trolox-LDH (a), IrganoxCOOH-LDH (b), and LDH-NO_3 (c)

Besides the characteristic stretching vibrations of the hydroxide layers [21], FT-IR spectra of IrganoxCOOH-LDH and Trolox-LDH (Figure 2) show absorptions due to the AO moieties (Figure S1, Supplementary Material) thus confirming the hybrid nature of both the systems. In particular, in the case of IrganoxCOOH-LDH the peak at 1543 cm^{-1} is assigned to the stretching vibration of the carboxylate group (C=O(O)-), whereas the absorption peaks ranging between 2960 and 2850 cm^{-1} arise from the $–CH_2$ and $-CH_3$ stretching vibrations of the hydrocarbon groups. The broad signal at 1630 cm^{-1}, partially overlapped with the absorption peak centered at 1543 cm^{-1}, is due to the bending vibration of crystal water. Similarly, the FT-IR spectrum of Trolox-LDH shows a peak at 1571 cm^{-1} which corresponds to the stretching vibration of the carboxylate group (C=O(O)-), whereas the absorptions at 2927 cm^{-1} and 2852 cm^{-1}, respectively, are due to the C-H stretching vibrations of $–CH_2$, $-CH_3$ and –CH groups of Trolox. The absorption band due to the crystal water is clearly visible also for this hybrid as well as a band at 1384 cm^{-1} due to the stretching vibration of the nitrate groups that had not been totally exchanged.

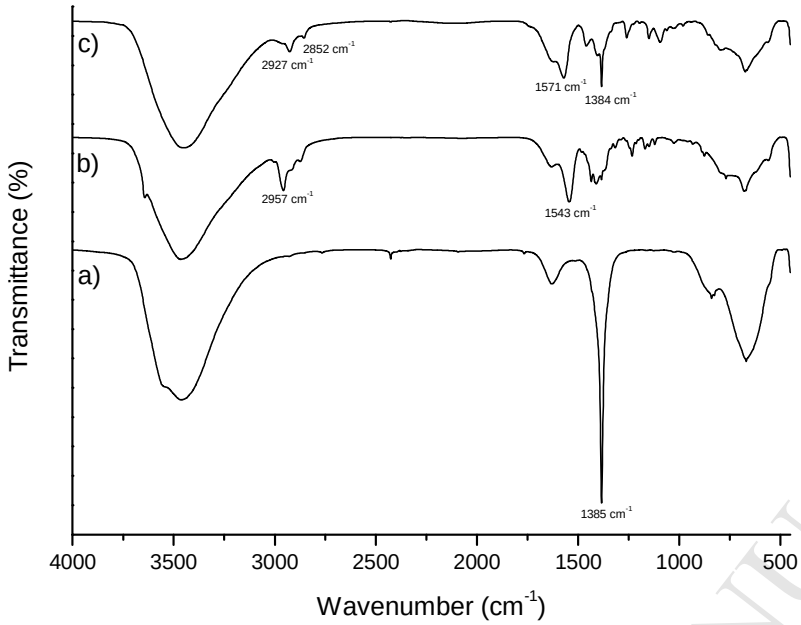

Figure 2. FT-IR spectra of a) LDH-NO_3, b) IrganoxCOOH-LDH, and c) Trolox-LDH

The TGA/DTG curves (collected under air flow) of LDH-NO_3, IrganoxCOOH-LDH, and Trolox-LDH are shown in Figure 3. The thermogram of LDH-NO_3 (Figure 3a) shows a two step decomposition process: an initial weight loss step, up to 150 °C, attributed to the loss of adsorbed and intercalated water, and a second weight loss step, between 250 and 700 °C attributed to the combined loss of the interlayer nitrate ions and to the dehydroxylation of the metal hydroxide layers [21]. The thermal decomposition of the two AO-LDHs (Figures 3b and 3c) mainly takes place in three steps. The first decomposition step, up to 180 °C, is due to the loss of the surface- and crystal-water molecules located in the interlayer region. In the temperature range between 180 and 800 °C, two main overlapping degradation steps are observed up to the formation of the metal oxides. This degradation stage is attributed to a succession of thermal processes: the decomposition of the intercalated AO molecules (180 - 260 °C), the loss of some unexchanged interlayer nitrate ions, and the dehydroxylation process of the layers. The amount of AO molecules anchored to the LDH was calculated taking into account the weight loss associated with the organic material decomposition. Accordingly, the quantity of intercalated AO anions was 26.1 wt.% for the IrganoxCOOH-LDH and 22.6 wt.% in the case of the Trolox-LDH. The chemical formula of the AO-LDHs is tentatively reported, assuming no change in the Al/Mg ratio:

IrganoxCOOH-LDH: $[Mg_{0.66}Al_{0.34}(OH)_2(NO_3)_{0.21}(C_{17}H_{25}O_3)_{0.13}]*0.56\ H_2O$

Trolox-LDH: $[Mg_{0.66}Al_{0.34}(OH)_2(NO_3)_{0.24}(C_{14}H_{18}O_4)_{0.10}]*0.25\ H_2O$

The moles of water per formula weight of compound were estimated by the first step of degradation of the TGA curve.

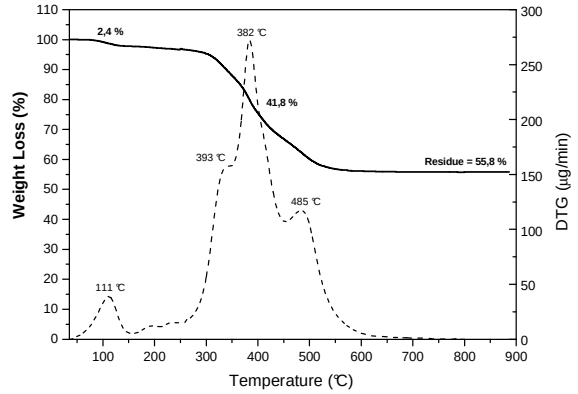

a)

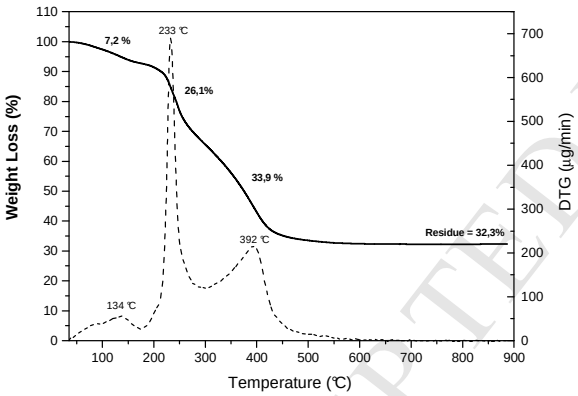

b)

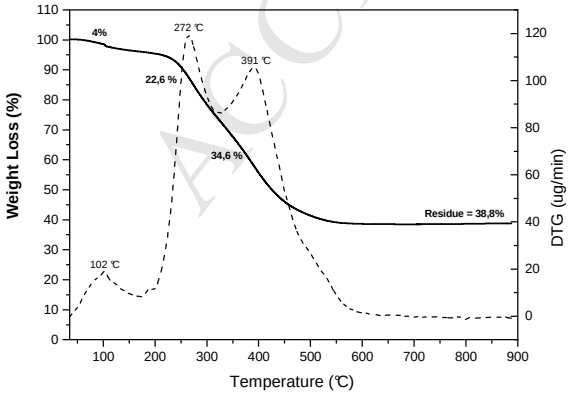

c)

Figure 3. TGA/DTG curves of a) LDH-NO_3, b) IrganoxCOOH-LDH, and c) Trolox-LDH

The antioxidant activity of AO-LDHs was determined with the DPPH method. The consumption of DPPH radicals in methanol solutions containing different concentration of the AO precursors (IrganoxCOOH and Trolox), BHT (used here as AO reference) and AO-LDHs was followed by UV-Vis spectroscopy applying a model based upon the steady state theory [34]. The analysis was carried out monitoring the absorbance of the band at 516 nm (of DPPH) versus time (Figure S2, Supplementary Material); the reduction in the 516 nm band is attributed to the reaction of the DPPH radical with the AO. To exclude that the absorbance decrease in the case of the AO-LDHs may be due to a possible adsorption of the DPPH onto the LDH layers, the organo-LDH having no antioxidant activity was reacted with DPPH. The absorbance decrease of this sample is comparable to that observed in the case of a solution of DPPH in methanol in the absence of AO (Figure S3, Supplementary Material).

The percentage of DPPH remaining at the steady state for different amounts of AO was determined and plotted against the AO/DPPH initial molar ratio (Figure S4, Supplementary Material). Accordingly, the effective concentration (EC_{50}) was determined (see Table 2).

Table 2. Effective Concentration (EC_{50}), antiradical power (ARP) and stoichiometry of the reaction between AO and DPPH

Antioxidant	EC_{50}	ARP ($1/EC_{50}$)	Stoichiometry
BHT	0.31±0.03	3.28±0.27	1.64±0.14
IrganoxCOOH	0.28±0.02	3.62±0.20	1.81±0.10
Trolox	0.25±0.02	4.06±0.26	2.03±0.13
IrganoxCOOH-LDH	0.13±0.01	7.72±0.60	3.86±0.30
Trolox-LDH	0.24±0.01	4.12±0.20	2.06±0.10

The results shown in Table 2 suggest that IrganoxCOOH-LDH has a higher DPPH activity compared to those of both BHT and IrganoxCOOH; indeed, it has a lower EC_{50} value, i.e. higher antiradical power (ARP). Accordingly, the stoichiometric value, which represents the number of moles of DPPH reduced by 1 mole of AO, is significantly higher for IrganoxCOOH-LDH than that for IrganoxCOOH. As a result, 1 mole of Irganox-COO^- anions intercalated into the LDH layers is able to reduce 4 moles of DPPH, whereas 1 mole of IrganoxCOOH can reduce only 2 moles of DPPH. Conversely, the DPPH activities of free Trolox and Trolox-LDH are comparable. Clearly, the anchoring of the IrganoxCOOH to the LDH layers appears to magnify the antioxidant activity of the AO.

The different behaviour observed for the pairs Trolox/Trolox-LDH and IrganoxCOOH/IrganoxCOOH-LDH can be tentatively explained considering the structure and reactivity of the AO precursors versus that of the carboxylate species intercalated between the LDH layers, as well as the geometrical effect due to the ionic bond between the AO moieties and the inorganic layers. It is, indeed, known that a good phenolic AO is generally characterized by a bond dissociation enthalpy (BDE) of the O-H bond lower than that necessary to break the O-H bond of the hydroperoxide formed during the inhibition reaction. Accordingly, it is possible that the AO acid precursors and the AO carboxylate species ionically bonded to the lamellae have a different a BDE. In the case of IrganoxCOOH-LDH the immobilization of the IrganoxCOO$^-$ carboxylate species between the lamellae may induce a change of the O-H BDE, thus giving rise to an increase in the antioxidant activity. On the contrary, the immobilization of Trolox as a carboxylate species between the LDH lamellae did not change too much its antioxidant activity, probably because having an alkoxyl group in the para position already has a very low BDE [41]. However, the observed behaviour can be also attributed to a simple geometrical effect because the AO molecules ionically linked to the LDH layers are well dispersed and not aggregated between them, thus favouring the reaction with the free radical species.

Interestingly, by plotting the DPPH absorbance versus time for solutions/suspensions containing a different concentration of AO species, it is clear that the reaction of IrganoxCOOH with DPPH is slower than that of IrganoxCOOH-LDH. The kinetics of DPPH consumption proceeded considerably faster for IrganoxCOOH-LDH than for IrganoxCOOH and BHT. Moreover, in the case of IrganoxCOOH-LDH a two-step behaviour was observed with a fast decay in the first minutes and then a slower decay step (Figure S5, Supplementary Material). Considering that the concentration of AO-LDH in the methanol suspensions was very low and that we tried to promote the delamination of the layers by sonicating the solutions (Tyndall effect, Figure S6, Supplementary Material), the reaction between the DPPH radicals and AO moieties anchored to the LDH layers is likely not to be controlled by diffusion. However, one cannot exclude the coexistence of single layers with intercalated and even aggregated structures that could affect the DPPH reaction with the AO moieties thus explaining the two-step behaviour.

3.2 Antioxidant stability of PLA/AO-LDH composites

Two PLA-based composites containing 0.5 wt.% of IrganoxCOOH-LDH and Trolox-LDH, respectively, were prepared by solution mixing (labelled as S) and melt extrusion (labelled as E) for comparison purposes (Table 1). The hybrid materials were first characterized by WAXD to investigate

the dispersion state of the filler. In all cases, the WAXD patterns showed the characteristic reflections of PLA crystals at 14.3, 16.7, 19.3, and 22.3°, which remain unchanged as compared with neat PLA (Figure 4 and Figure 5). In the range of 2θ=1.5-12° both PLA/IrganoxCOOH-LDH and PLA/Trolox-LDH, made by solution mixing and melt extrusion, did not show the (003) basal reflection of the fillers suggesting the loss of the ordered lamellar structure.

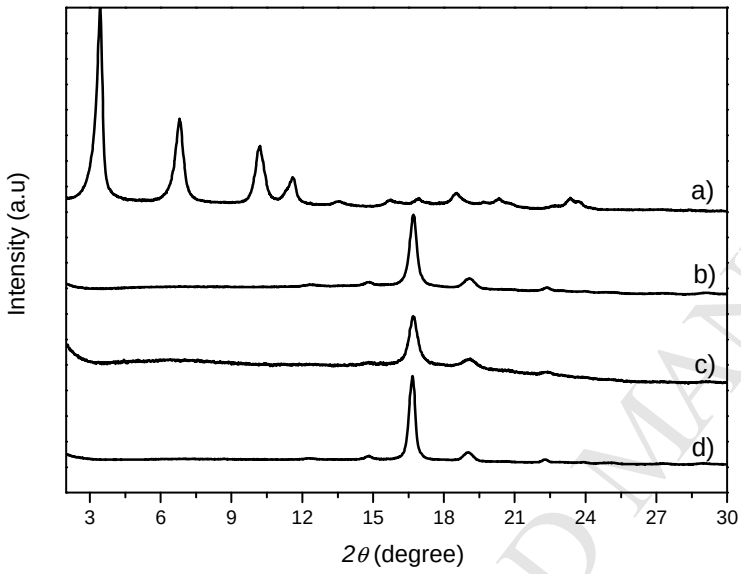

Figure 4. Comparison between WAXD patterns of a) IrganoxCOOH-LDH, b) PLA, c) PLA/IrganoxCOOH-LDH (S), and d) PLA/IrganoxCOOH-LDH (E)

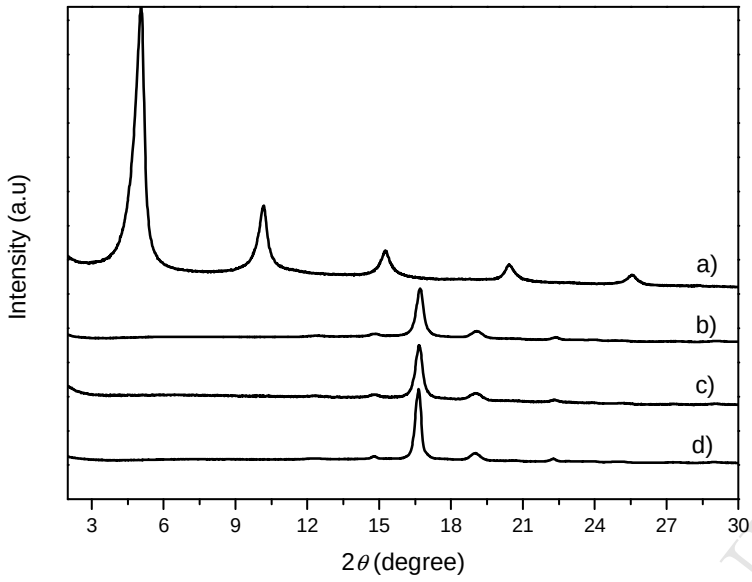

Figure 5. Comparison between WAXD patterns of a) Trolox-LDH, b) PLA b), c) PLA/Trolox-LDH (S), and d) PLA/Trolox-LDH (E)

However, even if the LDH concentration is too low to be meaningful for the assessment of an exfoliated morphology [42-44], the disappearance of the diffraction peaks suggests a disordered structure of the inorganic packing.

As a confirmation of the dispersion level, representative TEM micrographs of the PLA composites obtained by solution mixing (Figure S7, Supplementary Material) show that the AO-LDHs are dispersed disorderly within the matrix and that particles with average dimensions ranging from 50 to 300 nm can be observed. The high-magnification TEM images show that the largest particles are tactoids, made up of ordered lamellae, where polymer chains are likely to be intercalated.

In order to assess the influence of the AO-LDHs against the thermo-oxidative degradation of PLA, accelerated thermal oxidative experiments of all the PLA/AO-LDH composites were carried out by ageing the samples at 200 °C in an air oven for different times. Later, SEC analyses, before and after ageing, were carried out to evaluate the extent of PLA degradation (Table 3). For comparison, mixtures of PLA with the precursors of the AO-LDHs (i.e. IrganoxCOOH and Trolox), added to the polymer in equal amount (with respect to the amount of AO species present in the PLA/AO-LDH samples) were also prepared by solution mixing, aged and characterized. Further, a film of PLA containing 0.5 wt.%

of organo-LDH (PLA/organo-LDH) was prepared by solution mixing, aged and analyzed similarly by SEC (Table 3).

It was found that Mn and Mw of PLA solubilised in $CHCl_3$ are very close to those of virgin PLA (pellets), whereas PLA extruded at 170°C shows a lower Mw. Moreover, the results obtained show that the thermo-oxidative treatment of neat PLA gives rise to large reduction in its molecular weight (both Mn and Mw), see Table 3, together with an increase in the dispersity, whereas the decrease was lower upon the addition of free AOs, e.g. in PLA/IrganoxCOOH and PLA/Trolox (Table S1, Supplementary Material). This experimental evidence is consistent with a thermo-oxidative degradation of PLA (i.e. polymer chain scission) by free radical processes [45-47], which are much less probably in the presence of AOs, efficiently protecting hence the polymer.

Table 3. Molecular weight and distribution of PLA and PLA composites measured by SEC at different ageing time

Sample	Ageing time (min)	Mn (g mol^{-1})	Mw (g mol^{-1})	Mw/Mn	100[Mn(t)/Mn(0)-1][a] (%)	100[Mw(t)/Mn(0)-1][a] (%)
PLA2003D pellets	0	122000	203000	–	–	–
PLA (S)[b]	0	115000	205000	1.8	–	–
	60	109000	192000	1.8	-5	-6
	180	39000	94000	2.4	-66	-54
	360	18000	43000	2.4	-85	-79
PLA (E)	0	114800	193400	1.7	–	–
	60	79800	153600	1.9	-30	-21
	180	43100	85900	2.0	-62	-56
	360	24800	50900	2.1	-78	-74
	540	19700	42600	2.2	-83	-78
PLA/IrganoxCOOH-LDH (S)	0	113000	204000	1.8	–	–
	60	109000	191000	1.8	-4	-6
	180	91000	169000	1.9	-19	-17
	360	74000	148000	2.0	-35	-27
PLA/IrganoxCOOH-LDH (E)	0	90300	165800	1.8	–	–
	60	82900	146100	1.8	-8	-12
	180	74800	129800	1.7	-17	-22
	360	44400	90100	2.0	-51	-46
	540	38300	77800	2.0	-58	-53
PLA/Trolox-LDH (S)	0	123000	212000	1.7	–	–
	60	108000	196000	1.8	-12	-8
	180	84000	166000	2.0	-32	-22
	360	66000	135000	2.0	-46	-36
PLA/Trolox-LDH (E)	0	90800	167500	1.8	–	–
	60	74900	147900	2.0	-18	-12
	180	61500	121700	2.0	-32	-27
	360	38200	81500	2.1	-58	-51
	540	33800	72100	2.1	-63	-57

[a]100[Mn(0)/Mn(t)-1]% and 100[Mw(0)/Mn(t)-1]% represent the M_w and M_n loss (in percent) obtained after ageing (normalised to the unaged samples).
[b]This PLA sample was prepared by solubilizing the pellets in $CHCl_3$ and then evaporating the solvent.

A similar effect was also observed for the PLA/AO-LDH samples (Table 3 and Figure 6). Indeed, comparing the samples obtained by solution mixing, the decrease of Mn of PLA (S) after 6 h of ageing was 85%, whereas that of PLA/IrganoxCOOH-LDH (S) was only 35%, and, similarly, in the case of the sample PLA/Trolox-LDH (S) the decrease of Mn was limited to 46%. The organo-LDH is well

known [48, 49] to induce a detrimental effect on the stability of PLA; indeed, the degradation of PLA/organo-LDH (S) was faster than neat PLA (S) (Table S1); e.g. after 1 h of ageing, the Mn drops to 67% compared to the 5% drop for the neat polymer matrix.

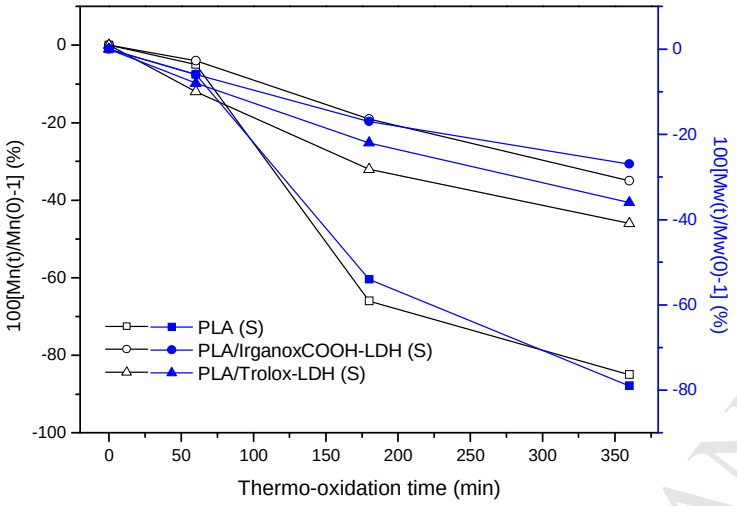

a)

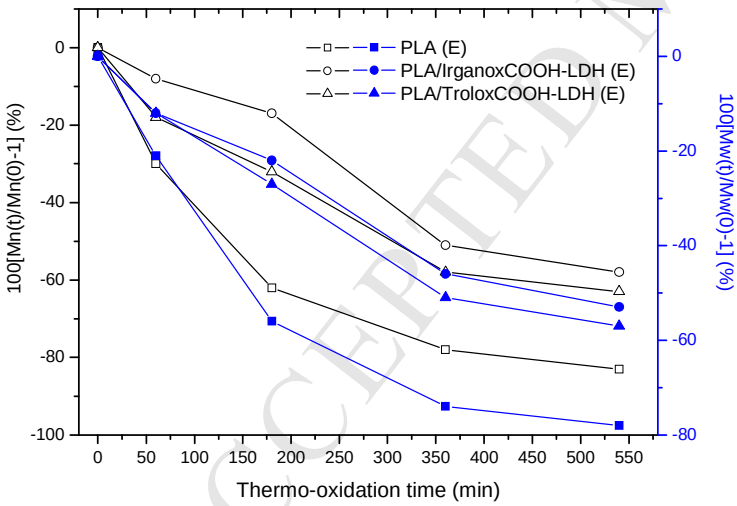

b)

Figure 6. Mn and Mw as a function of the ageing time at 200 °C for PLA, PLA/IrganoxCOOH-LDH, and PLA/Trolox-LDH made by solution mixing (a) and melt extrusion (b).

The addition of Trolox and IrganoxCOOH is seen to bring about a lower extent of change in the Mn value, i.e. lower level of degradation, after 6 h of ageing compared to that of the hybrid AO-LDHs in the PLA composites (Table S1).

Notably, the molecular weight of the samples prepared by melt extrusion, before the ageing process, is lower than that of the corresponding samples obtained by solution mixing. PLA is, indeed, reported to degrade during the thermal processing with LDHs and it seems that the degradation of the organo modifier accelerates the degradation of PLA causing a decrease of the melt viscosity and reasonably also of the molecular weight [50]. However, during the ageing of the extruded samples, the AO-LDHs seem to protect the matrix from additional degradation at least within the first 3 hours.

From these results, it appears that the immobilization/anchoring of the antioxidant moieties onto the LDH is efficient in protecting PLA from the thermo-oxidation, but the system appears less efficient compared to an analogous sample that contains a free AO. However, it is necessary to consider that the availability of the AO to protect the polymer depends on the morphology of the composites and on the proximity of the AO functionality to the polymer chains. Independently of the morphology, the anchoring of the AO to the inorganic layers lowers the AO mobility, presumably decreasing its activity.

Dynamic small strain amplitude oscillatory tests were also carried out to investigate the viscoelastic properties of PLA and PLA/AO-LDH (S) samples and to correlate the changes that occur at elevated temperature with changes in the molecular structure of PLA. It is indeed well known that the thermal degradation of PLA during processing leads not only to molecular weight reduction, but also to an overall reduction of rheological properties [51]. In particular, the greater the processing severity, the greater is the drop in both viscosity and modulus. The results (complex viscosity, storage and loss moduli as a function of frequency, Figure S8, Supplementary Material) suggest that the IrganoxCOOH-LDH exerts a stabilizing effect on the PLA matrix, i.e. resisting changes in its molecular weight, while Trolox-LDH appears to be less efficient under the same preparation conditions. However, the analysis also highlights that the AO-LDHs promote a reduction of complex viscosity, storage and loss moduli versus frequency with respect to neat PLA (S), which may be attributed to a slipping effect between the LDH layers in the macromolecular/layer-layer system [52].

To corroborate the outcomes of the thermal ageing experiments, the resistance of PLA and PLA/AO-LDH samples against thermally induced oxidation was also evaluated by determining the oxidation induction time (OIT) by DSC analysis [45, 53]. The results obtained show that the oxidation of neat PLA at 230 °C begins almost immediately (Figure S9, Supplementary Material) and that the presence of AO-LDHs in PLA prevents its oxidative degradation in the case of the samples prepared by solution mixing. For example, the OIT values (unaged, t = 0) of PLA/IrganoxCOOH-LDH (S) and PLA/Trolox-LDH (S) increased with respect to neat PLA by about 10 and 8 min, respectively (Table 4). A similar

behaviour was found in the case of PLA/IrganoxCOOH (S) and PLA/Trolox (S) albeit some differences were observed.

Table 4. OIT values at 230 °C of PLA, PLA/AO-LDH, and PLA/AO samples (S) and (E) before and after 12-months storage and migration test

Sample	OIT (min)		
	Time zero	After storage[a]	After migration test
PLA[b]	<1	<1	<1
PLA/IrganoxCOOH (S)	7.7 ± 1.7	7.4 ± 1.1	5.1± 1.1
PLA/IrganoxCOOH-LDH (S)	11.1 ± 2.9	11.4 ± 3.0	10.0 ± 1.8
PLA/Trolox (S)	13.2 ± 2.1	6.9 ± 0.9	2.9 ± 0.8
PLA/Trolox-LDH (S)	8.3 ± 1.0	8.0 ± 1.0	3.0 ± 0.7
PLA/organo-LDH[b]	<1	n.d.	n.d.

[a]The samples were stored at room temperature for 12 months.
[b]The oxidation of these samples began immediately after the switching of the gas from nitrogen to oxygen carried out at 230 °C.

The results confirm that the AO-LDHs are able to prevent the thermo-oxidative degradation of PLA and considering that the oxidation of PLA/organo-LDH started immediately after the purge gas was switched from nitrogen to oxygen, a barrier effect due to the LDH lamellae can be excluded.

Finally, in order to assess the non-releasing character and stability of the AO-LDHs embedded into PLA, preliminary migration tests were carried out on films of PLA/IrganoxCOOH-LDH (S) and PLA/Trolox-LDH (S), respectively. Accordingly, OIT values were determined after a period of natural ageing (the samples were stored at room temperature for 12 months) and after migration test of 24 h at 40 °C with ethanol/water 95/5 solution [40], and data were compared with those obtained for physical blends (PLA/IrganoxCOOH (S) and PLA/Trolox (S)). The data in Table 4 show that both storage and migration test caused a significant decrease in the OIT in the case of both PLA/IrganoxCOOH (S) and PLA/Trolox (S), which is most likely due to the release of the free AOs. In contrast, the OIT values calculated for the two PLA/AO-LDH (S) composites after 12-months storage are almost unchanged with respect to those obtained for fresh (untreated) samples, thus evidencing the retention of the host-guest systems. However, the two composites behaved differently under contact with the aqueous alcoholic solution: in the case of PLA/IrganoxCOOH-LDH (S), the OIT after the migration test was similar to that of the untreated sample, whereas in case of PLA/Trolox-LDH (S) the test caused a

consumption of the stabilizer and a decrease of the OIT. Considering that both Trolox and IrganoxCOOH are soluble in ethanol/water 95/5 and that both migrate from their respective PLA physical blend, the difference observed might be due to the different stability of the AO-LDHs, which in turn depends on the nature of the simulating liquid and on the ionic bond/interactions between the AO molecules and LDH layers. This process is also limited by diffusion-controlled conditions depending on the morphology of composites. Moreover, even if the WAXD analysis demonstrated that the AO moieties are intercalated in the AO-LDHs, it cannot be excluded that a part of the organic fraction is only adsorbed and, accordingly, it can easily migrates changing the antioxidant capability and then the OIT of the sample. Finally, the migration of lamellae can also occur, as previously reported [40].

4. Conclusions

Two different AO-LDH host-guest systems were successfully prepared by intercalating between the inorganic layers a hindered phenol containing molecule (IrganoxCOOH) and, for what we believe was the first time, a water-soluble analogue of vitamin E (Trolox) as a natural AO. In both cases, i.e. for hybrids (IrganoCOOH-LDH and Trolox-LDH), it was found that the DPPH free radical scavenging capacity of the free AOs was maintained and even improved in the case of IrganoxCOOH-LDH.

Two PLA composites containing 0.5 wt% of IrganoxCOOH-LDH and Trolox-LDH, respectively, were obtained by solution mixing and melt extrusion. Films of these samples were subjected to controlled ageing at 200 °C under air for different time intervals, and the specimens were analyzed by SEC. PLA chains undergo thermo-oxidative degradation, with a severe reduction of molecular weight and an increase in dispersity. The molecular weight results in this work indicate clearly that the AO-LDHs ~~are~~ have been successful in protecting the polymer from thermo-oxidative degradation. In addition, the OIT values at 230 °C for PLA/IrganoxCOOH-LDH (S) and PLA/Trolox-LDH (S) increased to about 10 and 8 times that of the neat PLA, respectively, thereby corroborating the beneficial effects observed for the AO-LDHs, if the molecular weight of the matrix is preserved. Finally, a preliminary migration test was explored to assess the non-releasing character of the AO-LDHs embedded into PLA. These initial results indicate that the AO-LDH hybrids have a low tendency to migrate compared to AO within PLA, due to a robust ionic anchoring of AO between the LDH layers, and thus keeping the AO protected inside the inorganic layers and active for a longer time. More detailed work on the migration of these AO-LDH will be done in future work.

Acknowledgements

This work was supported by Italian Ministry of University and Research (MIUR) under the program FIRB 2010 - Futuro in Ricerca. Project title: "GREENER-Towards multifunctional, efficient, safe and stable 'green' bio-plastics based nanocomposites of technological interest via the immobilization of functionalized nanoparticles and stabilizing molecules" (Project cod: RBFR10DCS7). The authors gratefully acknowledge Dr. Gennaro Gentile (Istituto per i Polimeri, Compositi e Biomateriali (IPCB), Consiglio Nazionale delle Ricerche) for acquiring TEM images.

References

1. P. Gijsman. Handbook of Environmental Degradation of Materials, Second Edition, 673-714 (2012). M. Kutz, Handbook of environmental degradation of materials, William Andrew Pub, Norwich, NY (2005).
2. S. Ray, R. P. Cooney. Thermal Degradation of Polymer and polymer Composites. In Handbook of Environmental Degradation of Materials, 2nd ed., M. Kutz., Ed., Elsevier: Oxford, UK (2012)
3. J. Murphy in "Additives for Plastics Handbook", Second Edition, Elsevier Advanced Technology, Oxford UK (2001)
4. X. Gao, G. Hu, Z. Qian, Y. Ding, S. Zhang, D. Wang, M. Yang, Polymer 48 (2007) 7309-7315
5. M. Bertoldo, F. Ciardelli, Polymer 45 (2004) 8751-8759
6. S. Al-Malaika, A. Golovoy, C. A. Wilkie in "Chemistry and technology of polymer additives". Oxford: Blackwell Science Ltd.; 1999
7. S. Beer, I. Teasdale, O. Brueggemann, Eur. Polym. J. 49 (2013) 4257-4264
8. P. Stagnaro, G. Mancini, A. Piccinini, S. Losio, M. C. Sacchi, C. Viglianisi, S. Menichetti, A. Adobati, S. Limbo, J. Polym. Sci. B Polym. Phys. 51 (2013) 1007-1016
9. S. Al-Malaika, N. Suharty, Polym. Degrad. Stab. 49 (1995) 77-89
10. T. H. Kim, N. Lee, Bull. Korean Chem. Soc. 24 (2003) 1809-1813
11. T. H. Kim, J. Appl. Polym. Sci. 94 (2004) 2117-2122.
12. T. H. Kim, DR. Oh, Polym. Degrad. Stab. 84 (2004) 499-503.
13. S. Al-Malaika, Adv. Polym. Sci. 169 (2004) 121-150
14. X. Gao, X. Meng, H. Wang, B. Wen, Y. Ding, S. Zhang, M. Yang, Polym. Degrad. Stab. 93 (2008) 1467-1471.
15. J. Chen, M. S. Yang, S. M. Zhang, Composites: A 42 (2011) 471-477.

16. N. Tz. Dintcheva, S. Al-Malaika, E. Morici, Polym. Degrad. Stab. 122 (2015) 88-101.
17. X. Shi, J. Wang, B. Jiang, Y. Yang, Polymer 54 (2013) 1167-1176.
18. R. M. Lucente-Schultz, V. C. Moore, A. D. Leonard, B. K. Price, D. V. Kosynkin, M. Lu, R. Partha, J. L. Conyers, J. M. Tour, J. Am. Chem. Soc. 131 (2009) 3934-3941.
19. G. G. C. Arizaga, K. G. Satyanarayana, F. Wypych, Sol. State Ion. 178 (2007) 1143–1162.
20. F. Ciardelli, S. Coiai, E. Passaglia, A. Pucci, G. Ruggeri, Polym. Int. 57 (2008) 805–836.
21. N. Muksing, R. Magaraphan, S. Coiai, E. Passaglia, eXPRESS Polym. Lett. 5 (2011) 428-448.
22. M. Silion, D. Hritcu, G. Lisa, M. I. Popa J. Porous Mater 19 (2012) 267-276.
23. X. Gao, L. Lei, D. O'Hare, J. Xie, P. Gao, T. Chang, J. Solid. State Chem. 203 (2013) 174-180.
24. X. Kong, L. Jin, M. Wei, X. Duan, Appl. Clay Sci. 49 (2010) 324-329.
25. J-H. Choy, Y-H. Son, Bull. Korean Chem. Soc. 25 (2004) 122-126.
26. E. Lima, J. Flores, A. S. Cruz, G. Leyva-Gomez, E. Krotzsch, Microp. Mesop. Materials 181 (2013) 1-7.
27. C. Rossi, A. Schoubben, M. Ricci, L. Perioli, V. Ambrogi, L. Latterini, G. G. Aloisi, A. Rossi, Int. J. Pharm. 295 (2005) 47-55.
28. C. Coelho, M. Hennous, V. Verney, F. Leroux, RSC Adv. 2 (2012) 5430-5438.
29. Y. Feng, Y. Jiang, Q. Huang, S. Chen, F. Zhang, P. Tang, D. Li. Ind. Eng. Chemical Research, 53 (2014) 2287−2292.
30. S. P. Lonkar, A. Leuteritz, G. Heinrich, RSC Adv. 3 (2013) 1495-1501.
31. S. P. Lonkar, B. Kutlu, A. Leuteritz, G. Heinrich, Appl. Clay Sci. 71 (2013) 8–14.
32. D. Rasselet, A. Ruellan, A. Guinault, G. Miquelard-Garnier, C. Sollogoub, B. Fayolle, Eur. Polym. J. 50 (2014) 109–116.
33. F. D. Kopinke, M. Remmler, K. Mackenzie, M. Moder, O. Wachsen, Polym. Degrad. Stab. 53 (1996) 329-342.
34. K. Mishra, H. Ojha, N. Kumar Chaudhury, Food Chem. 130 (2012) 1036–1043.
35. S. Coiai, E. Passaglia, A. Hermann, S. Augier, D. Pratelli, R. C. Streller, Polym. Comp. 31 (2010) 744-754.
36. S. Coiai, M. Scatto, L. Conzatti, F. Azzurri, L. Andreotti, E. Salmini, P. Stagnaro, A. Zanolin, F. Cicogna, E. Passaglia, Polym. Adv. Technol. 22 (2011) 2285-2294.
37. S. C. Carroccio, G. Curcuruto, N. Tz. Dintcheva, C. Gambarotti, S. Coiai, G. Filippone, Rapid Commun. Mass Spectrom. 27 (2013) 1359–1366.
38. Z. Liu, R. Ma, M. Osada, N. Iyi, Y. Ebina, K. Takada, T. Sasaki, J. Am. Chem. Soc. 128 (2006)

4872-4880.

39. X. Lu, L. Meng, H. Li, N. Du, R. Zhang, W. Hou, Mater. Res. Bull. 48 (2013) 1512–1517.
40. B. Schmidt, V. Katiyar, D. Plackett, E. H. Larsen, N. Gerds, C. Bender Koch, J. H. Petersen, Food Addit. Contam. Part A 28 (2011) 956-966.
41. M Lucarini, GF. Pedulli, Chem. Soc. Rev. 39 (2010) 2106-2119.
42. R. A. Vaia, E. P. Giannelis, Macromolecules 30 (1997) 8000-8009.
43. R. A. Vaia, E. P. Giannelis, Macromolecules 30 (1997) 7990- 7999.
44. A. C. Balazs, C. Singh, E. Zhulina, Macromolecules 31 (1998) 8370-8381.
45. G. Gorrasi, A. Sorrentino, Polym. Degrad. Stab. 98 (2013) 963-971.
46. E. Ikada, J. Photopolym. Sci. Technol. 10 (1997) 265-269.
47. E. Ikada, J. Photopolym. Sci. Technol. 12 (1999) 251-256.
48. V. Katiyar, N. Gerds, C. B. Koch, J. Risbo, H. C. B. Hansen, D. Plackett, J. Appl. Polym. Sci. 122 (2011) 112-125.
49. N. Gerds, V. Katiyar, C. B. Koch, H. C. B. Hansen, D. Plackett, E. H. Larsen, J. Risbo, Polym. Degrad. Stab. 97 (2012) 2002-2009.
50. R. Scaffaro, L. Botta, E. Passaglia, W. Oberhauser, M. Frediani, L. Di Landro, Polym. Eng. Sci. 54 (2014) 1804-1810.
51. R. Al-Itry, K. Lamnawar, A. Maazouz, Polym. Degrad. Stab. 97 (2012) 1898-1914.
52. X. Wang, Q. Zhang, Polym Int. 53 (2004) 698-707.
53. M. Schmid, S. Affolter, Polym. Test. 22 (2003) 419–428.